Histologic Evidence of a Connective Tissue Attachment to Laser Microgrooved Abutments: A Canine Study

Myron Nevins, DDS[1]/David M. Kim, DDS, DMSc[2]
Sang-Ho Jun, DDS, MS[3]/Kevin Guze, DMD[4]
Peter Schupbach, PhD[5]/Marc L. Nevins, DMD, MMSc[6]

Previous research has demonstrated the effectiveness of laser-ablated microgrooves placed on implant collars to support direct connective tissue attachments to altered implant surfaces. Such a direct connective tissue attachment serves as a physiologic barrier to the apical migration of the junctional epithelium and prevents crestal bone resorption. The current prospective preclinical trial sought to evaluate bone and soft tissue healing patterns when laser-ablated microgrooves were placed on the abutment. A canine model was selected for comparison to previous investigations that examined the negative bone and soft tissue sequelae of the implant-abutment microgap. The results demonstrate significant improvement in peri-implant hard and soft tissue healing compared to traditional machined abutment surfaces. (Int J Periodontics Restorative Dent 2010;30:245–255.)

[1]Associate Clinical Professor, Division of Periodontology, Department of Oral Medicine, Infection and Immunity, Harvard School of Dental Medicine, Boston, Massachusetts.
[2]Assistant Professor, Division of Periodontology, Department of Oral Medicine, Infection and Immunity, Harvard School of Dental Medicine, Boston, Massachusetts.
[3]Research Fellow, Department of Plastic and Oral Surgery, Children's Hospital Boston, Boston, Massachusetts.
[4]Research Fellow, Division of Periodontology, Department of Oral Medicine, Infection and Immunity, Harvard School of Dental Medicine, Boston, Massachusetts.
[5]PSchupbach Histology, Research Laboratory, Biomaterials, Horgen, Switzerland.
[6]Assistant Clinical Professor, Division of Periodontology, Department of Oral Medicine, Infection and Immunity, Harvard School of Dental Medicine, Boston, Massachusetts.

Correspondence to: Dr Myron Nevins, Harvard School of Dental Medicine, 188 Longwood Avenue, Boston, Massachusetts 02115; email: nevinsperimp@aol.com.

The preservation of stable relationships between overlying soft tissues and the underlying supporting crestal bone is critical for optimal form and function in implant-supported restorations. Such morphologic stability is particularly important in the anterior esthetic zone of the maxilla, where the anatomical integrity of esthetically critical marginal and papillary tissues is intimately dependent on stable crestal bone levels. Unfortunately, loss of crestal bone, or "dieback," to the first coronal implant thread is commonly observed following abutment attachment, resulting in an average of 1.5 to 2.0 mm of bone loss after the first year in function, often followed by an ongoing 0.1-mm loss each year thereafter.[1–7]

The relationship between the implant-abutment junction (IAJ) and implant-related crestal bone loss has received increased attention and concern.[1,4,8–11] Preclinical trials using a canine model have confirmed a 3-mm dimension of the peri-implant soft tissues.[1–4] The microgap created at the IAJ consistently resulted in an inflammatory infiltrate that drove the healthy peri-implant connective

tissue component apically, resulting in at least 1.5 to 2 mm of crestal bone loss.[1,12]

Preclinical and clinical studies have been conducted to reduce or minimize crestal dieback by examining the role that microchannels, with defined three-dimensional shapes and depths, might play in controlling fibroblastic and osteoblastic behavior by limiting the apical migration of the junctional epithelium.[13,14] The significant results of a prospective proof-of-principle human histologic study demonstrated direct connective tissue attachment to precisely generated Laser-Lok microgrooves on the implant collar.[15] This raises the question of whether similar results would occur if configured laser-ablated microgrooves were placed on the abutment surface. Such an altered surface, unlike traditional machined-surface abutments, might provide improved opportunities for a direct fibrocollagenous attachment and thus potentially limit the apical epithelial migration that is common in more traditional abutment-implant complexes. In addition, direct connective tissue attachment to the abutment surface may potentially mitigate or altogether eliminate the negative sequelae secondary to microbial leakage from the IAJ microgap, thereby reducing the potential for peri-implant crestal bone loss.

The purpose of the current preclinical proof-of-principle study was to determine whether precisely configured Laser-Lok microgrooves placed within a defined healing abutment region prevent or reduce crestal bone loss when compared to a machined abutment, and to determine the tissue attachments occurring at the micro-grooved abutment surface during healing through histologic, micro–computed tomographic (micro-CT), and scanning electron microscopic (SEM) analyses.

Method and materials

The current study, which was approved under the Institutional Animal Care and Use Committee protocol, was designed to examine the effects of two different implant and abutment surfaces on epithelial and connective tissue attachment, as well as peri-implant bone levels. The sites were randomly assigned to receive tapered internal implants (BioHorizons) with either resorbable blast texturing (RBT) or RBT with a 0.3-mm machined collar (Fig 1a). Each implant was 3.8 mm in diameter and 9.0 mm in length. In addition, either machined-surface or Laser-Lok 8-µm microchannel healing abutments were assigned randomly to each implant, with the Laser-Lok microchannels applied to a 0.7-mm-tall band located immediately coronal to the IAJ or microgap (Fig 1b). The width of the band evaluated was the same dimension as the portion of the band on the Laser-Lok implant that comes into contact with the soft tissue. The abutments were placed at the time of surgery.

Six foxhounds, each weighing at least 25 kg, were selected for this study. Each dog received 6 implants in the bilateral mandibular premolar and first molar extraction sites, for a total of 36 implants for six dogs. Figure 2 describes the four cohorts (groups A,

Fig 1a (left) *Resorbable blast texturing (RBT) implant with a 0.3-mm machined collar (left) and an RBT implant without the machined collar (right).*

Fig 1b (right) *Healing abutment with a 0.7-mm Laser-Lok microgrooved zone (left) and fully machined abutment without the laser-ablated microgrooves (right).*
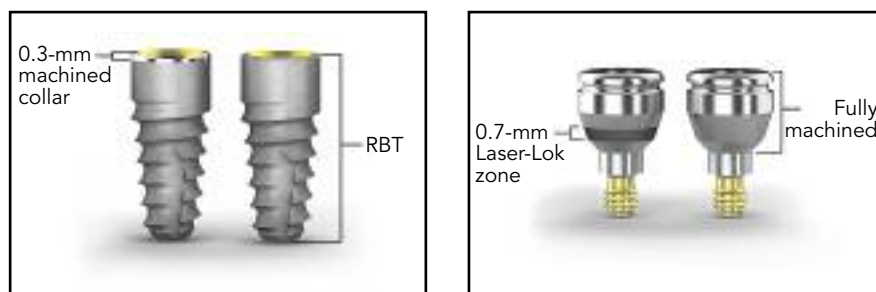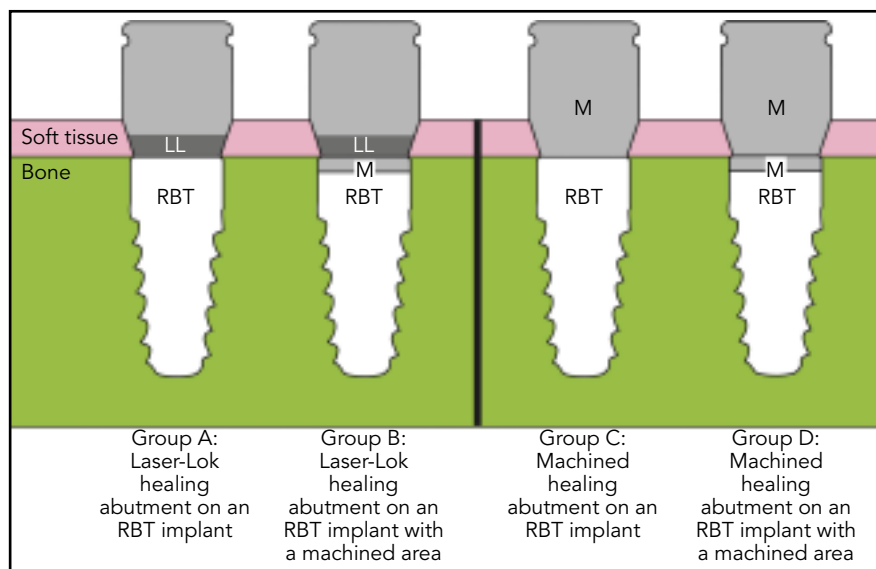

Fig 2 (right) *The four cohorts. LL = Laser-Lok; RBT = resorbable blast texturing; M = machined surface.*

B, C, and D) included in this study. Each group received 9 implants.

Surgical extraction phase

Full-thickness flaps were reflected under 10 to 12 mL of thiopental sodium (Pentothal, Hospira) and local anesthesia via 2% lidocaine with 1:100,000 epinephrine for the bilateral removal of the four mandibular premolars and first molars. The flaps were coapted and sutured without tension with multiple 4.0 chromic gut interrupted sutures (Ethicon).

Each foxhound received 1 g of cefazolin (Apotex), intravascularly or intramuscularly, every 3 days for the first week postoperative. Postoperative pain was managed with 0.3 mg of buprenorphine HCl (Reckitt Benckiser Healthcare) intramuscularly once every 12 hours for the first 48 hours.

Surgical implant placement

Crestal incisions were made and full-thickness mucoperiosteal flaps were reflected 45 days postextraction. Three implants per side were inserted into each animal according to a randomized distribution pattern generated prior to surgery. No two adjacent implants were of the same type. Implant osteotomies were performed with torque-reducing rotary instruments at 500 rpm using a sterile saline solution. All implants were placed according to manufacturer guidelines. Every effort was made to place the implant platforms level with the osseous crest to allow for an accurate histologic and micro-CT assessment of crestal bone levels (Fig 3). Laser-Lok microchanneled healing abutments and standard machined surface healing
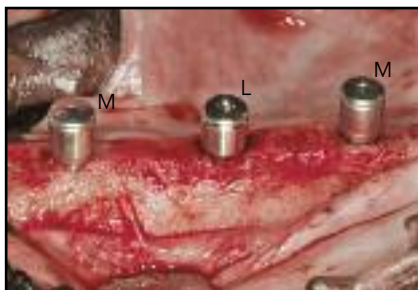
Fig 3 (left) *Implant platforms were placed as level as possible with the osseous crest to allow for accurate histologic and micro-CT assessment of crestal bone levels.*

Fig 4 (right) *A Laser-Lok microgrooved healing abutment* (L) *and standard machined-surface healing abutments* (M) *were placed on the implants at the time of implant placement.*

abutments were connected to the implants (Fig 4) following a randomized distribution pattern. Mucoperiosteal flaps were closed tension-free and sutured with multiple expanded poly-tetrafluoroethylene interrupted and horizontal mattress sutures (Gore-Tex, W. L. Gore). All sutures were removed within 2 weeks.

All six foxhounds received a soft diet for the duration of the 3-month healing period. At 3 months following implant surgery, all six foxhounds were sacrificed. Each mandible was resected en bloc and placed immediately in fixative for histologic preparation and evaluation.

Specimen preparation and analysis

Micro–computed tomography
The specimens were scanned using a high-resolution micro-CT system (µCT 40, Scanco Medical) in multislice mode. Each image data set consisted of approximately 600 micro-CT slice images. The specimens were scanned in high resolution with an x-, y-, and z-resolution of 16 µm. The image data sets were used to produce three-dimensional views of the specimens using special software (Scanco Medical), creating high-resolution images of bone-to-implant contact.
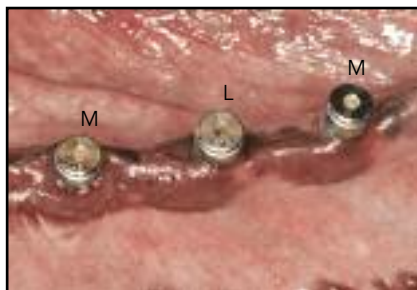
Light microscopy
Fixed samples were dehydrated in a graded series of ethanols using a dehydration system with agitation and a vacuum. The blocks were infiltrated with Kulzer Technovit 7200 VLC resin. Infiltrated specimens were placed into embedding molds, and polymerization was performed under ultraviolet light. Polymerized blocks were sectioned in a mesiodistal direction and parallel to the long axis of each implant. The slices were reduced by microgrinding and polishing using an Exakt grinding unit to an even thickness of 30 to 40 µm. Sections were stained with toluidine blue–Azure II and examined using both a Leica MZ16 stereomicroscope and a Leica 6000DRB light microscope.

Scanning electron microscopy
Specimens intended for SEM were dehydrated through a graded series of acetones and dried by the critical point method[16] using carbon dioxide as a transitory fluid. Specimens were examined in a scanning electron microscope.

Fig 5 *At the end of 3 months, the peri-implant mucosa appeared normal with little evidence of inflammation around the Laser-Lok microgrooved* (L) *and standard machined-surface* (M) *healing abutments.*

Results

All test and control implants were successfully osseointegrated at the time of the 3-month sacrifice. Peri-implant mucosal soft tissue healing proceeded uneventfully with little evidence of inflammation (Fig 5). No evidence of localized infection was present throughout the entire 3-month healing period at any of the implant sites. The unintentional loss of 11 abutments, a result of the animals chewing on their cages, reduced the number of available abutments to study. The resulting lower number precluded a meaningful quantitative analysis.

Group A

Histologic observations

The peri-implant soft tissues consisted of an epithelial barrier composed of sulcular epithelium merging with junctional epithelium (JE). A discrete, supracrestal connective tissue barrier was seen in all group A sites apical to the JE (Fig 6a).

The JE ended at the coronal-most position of the abutment's Laser-Lok microchannels, where a zone of connective tissue fibers was seen perpen-dicular to the microgrooved band. There was coronal bone attachment to the microchannel abutment surface apical to the perpendicularly oriented CT fibers in two group A specimens (Figs 6b and 6c). The IAJ-mediated microgap was thus eliminated by bone-implant contact coronal to the IAJ (Figs 6b to 6e). Importantly, a long JE was not observed in group A histologic sections.

Micro-CT and SEM observations

Micro-CT examination corroborated the histologic findings. Intimate bone-to-implant contact was seen extending onto the RBT implant collar (Fig 6f).

SEM analysis demonstrated intense connective tissue networks attached to the entire laser-ablated abutment surfaces (Fig 6g). This appeared to serve as an impenetrable barrier to apical migration of the JE. The normal circumferentially oriented collagen fibers were noted to inter-digitate with the previously mentioned perpendicularly oriented connective tissue fibers.
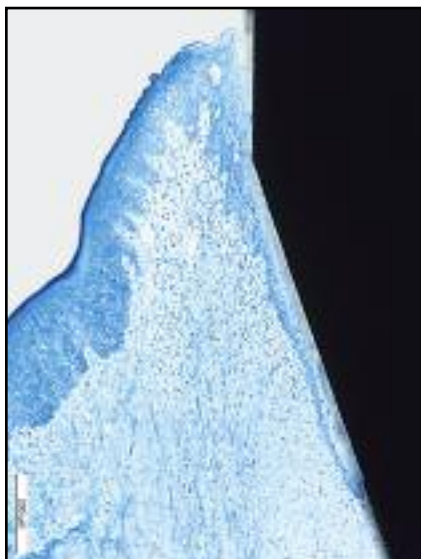
Fig 6a *At group A sites, the JE ended at the coronal-most Laser-Lok grooved area. Apical to the JE, healthy connective tissue fibers attached perpendicularly to the laser-ablated channels.*
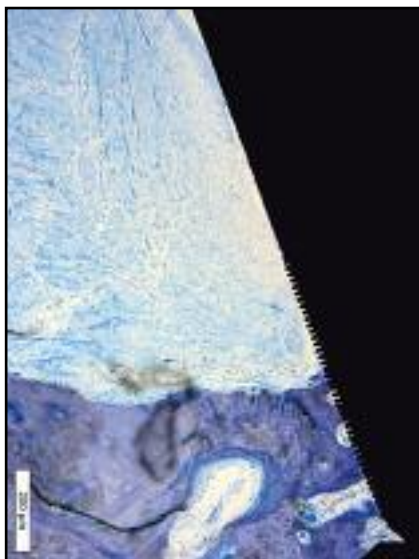

Fig 6b *In this group A specimen, regenerated bone was attached to the Laser-Lok abutment surface and the IAJ microgap was eliminated.*
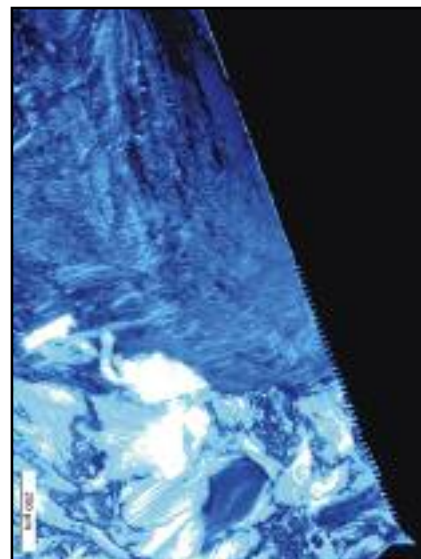

Fig 6c *A polarized light image demonstrates perpendicularly inserting connective tissue fibers into the microgrooved abutment surface.*

Fig 6d (left) *Light microscopic view of a group A specimen demonstrating bone-to-implant contact.*
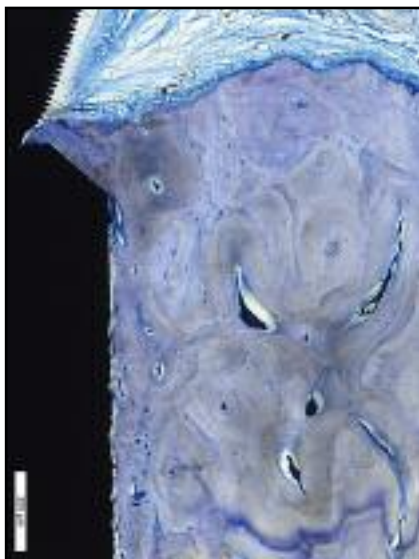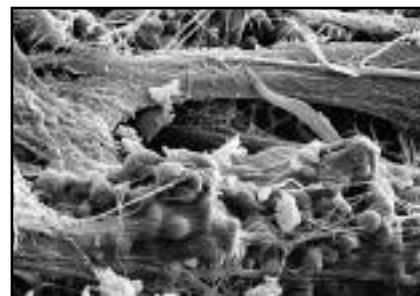
Fig 6e (right) *A high-power view of Fig 6d demonstrates bone regeneration at the IAJ interface, effectively eliminating the IAJ microgap.*

Fig 6f (left) *Micro-CT of a group A specimen corroborates the light microscopic findings, including excellent bone-to-implant contact up to the IAJ. No crestal bone resorption occurred.*

Fig 6g (right) *Intense fibroblastic cellular activity occurred at the Laser-Lok microgrooved areas in all group A specimens. Dense networks of connective tissue fibers can be seen attached to the laser-ablated microchannels.*

Group B

Histologic observations

The epithelial peri-implant soft tissues were identical to those seen in group A. The JE terminated at the coronal-most position of the Laser-Lok abutment microgrooves (Fig 7a). Functionally oriented, perpendicularly directed connective tissue fibers were juxtaposed intimately against the entire band of the Laser-Lok microchannels (Fig 7b). Apical to this band of connective tissue fibers, newly regenerated bone was seen osseointegrating with the machined collar of the RBT implants. No group B site exhibited apical migration of the JE.

SEM observations

Ultrastructural examination of group B specimens proved identical to group A SEM findings. Dense masses of interlacing connective tissue fibers occupied all surfaces of the Laser-Lok microchannels (Fig 7c).

Group C

Histologic observations

Apical migration of the JE was demonstrated in some group C sites (Fig 8a). The imposition of a long JE along the abutment and implant collar surfaces (Fig 8b) prevented connective tissue fibers from forming the protective barrier and may be responsible for a more apical bone level.

SEM observations

Group C ultrastructural views demonstrated an almost complete lack of connective tissue fiber attachment to either the abutment or implant surfaces (Fig 8c). No regenerated bone was seen apposed to either the abutment or implant collar surfaces. Significantly, the IAJ microgap remained exposed to the surrounding environment.
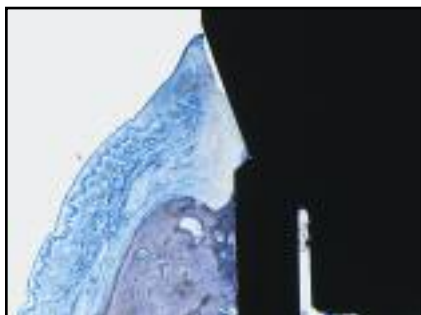
Fig 7a *Group B specimens demonstrated native and new bone (darker stain) on the implant surface. This probably is the result of the correction of drilling disparity, but it is evidenced that the supracrestal connective tissue fiber has prohibited apical migration of epithelium, allowing the bone to respond in an aseptic environment.*
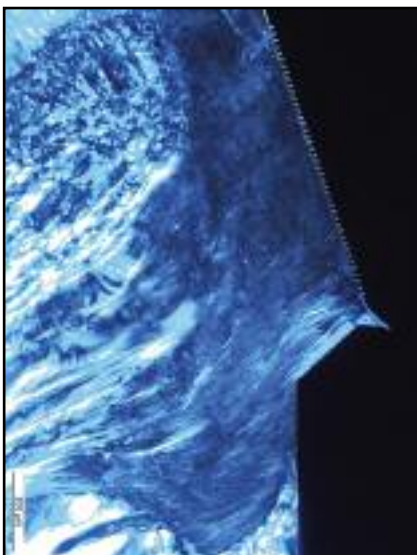

Fig 7b *Group B specimen demonstrating perpendicularly oriented connective tissue fibers against the entire surface of the Laser-Lok grooved area.*
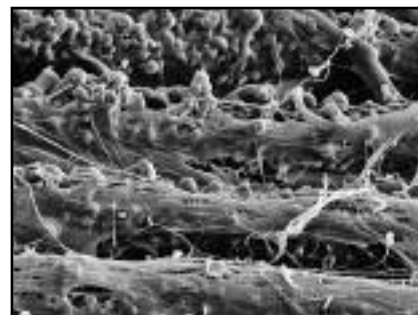

Fig 7c *SEM image of group B specimen demonstrated intense fibroblastic activity at the laser grooved surfaces, resulting in a dense network of interlacing connective tissue fibers that served as a natural barrier to apical epithelial migration.*
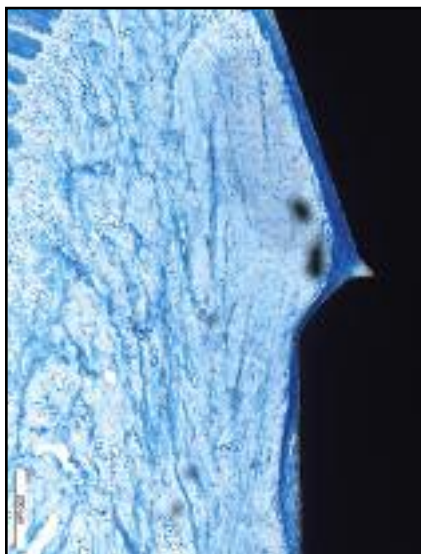

Fig 8a *A long JE is seen along the abutment and implant collar surfaces, preventing connective tissue fibers from forming the protective barrier seen in groups A and B.*
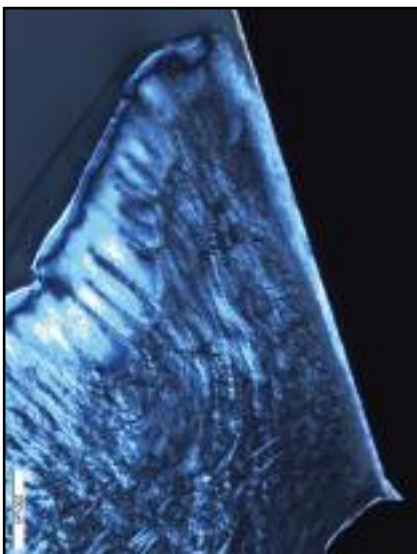

Fig 8b *A polarized light image of a group C site demonstrates connective tissue fibers parallel to the machined healing abutment with no evidence of perpendicularly inserting connective tissue fibers.*

Fig 8c *An SEM of a group C specimen showing no connective tissue fiber attachment to either the abutment or implant surfaces. The IAJ microgap remains exposed to the surrounding tissue bed.*
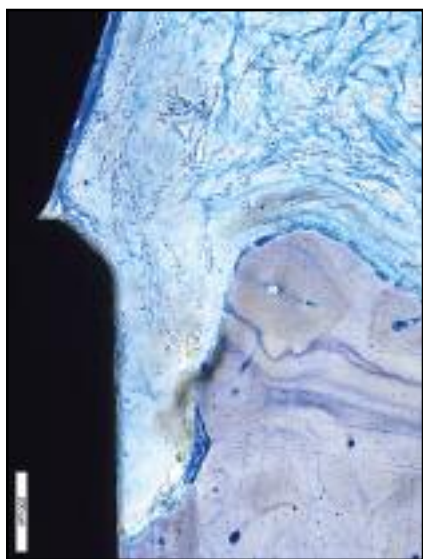
Fig 9a *A group D high-power specimen demonstrated apical JE migration, resulting in significant crestal bone resorption.*
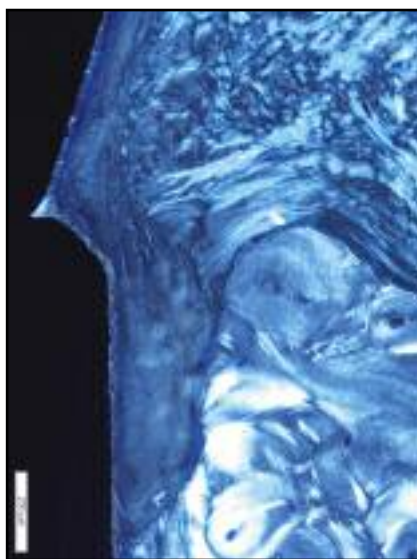

Fig 9b *In a polarized light view, this group D site clearly demonstrates parallel running connective tissue fibers against both the abutment and implant collar surfaces. In addition, significant crestal bone loss is seen.*

Fig 9c *As in group C, SEM imagery demonstrated the almost total absence of connective tissue fibers covering either the healing abutment or implant collar surfaces. The IAJ microgap remained exposed to the surrounding tissue bed.*

Group D

Histologic observations

The absence of Laser-Lok microchannels resulted in apical migration of the JE and some crestal bone loss (Fig 9a). The imposition of a long JE extending to the alveolar crest consistently resulted in connective tissue fibers parallel to the abutment and implant surfaces (Fig 9b).

SEM observations

Similar ultrastructural findings seen at group C sites were also seen in group D specimens. Minimal connective tissue attachment was demonstrated at the abutment or implant surfaces. The SEM imagery revealed an IAJ covered with neither connective tissue fibers nor bone, exposing the critically important microgap to the surrounding environment (Fig 9c).

Discussion

Commonly observed crestal bone resorption, or "dieback," to the first coronally positioned implant thread following abutment attachment threatens the needed balance between the stable underlying bone and overlying soft tissues. Multiple causes of such undesirable crestal bone resorption have been suggested, including the inherent need for a minimum biologic width dimension, as seen in the natural dentition, and the bacterial and inflammatory cell infiltrate present at the IAJ microgap.[1,6,7] This inflammatory cell–laden connective tissue adjacent to the IAJ microgap forces the repositioning of noninflamed peri-implant connective tissue and the crestal bone apically. The relatively constant spatial relationship between the IAJ and the alveolar crest confirms the approximate 1.5- to 2-mm apical position of the bony crest relative to the implant-abutment interface.[3,17,18]

Laser-ablated microgrooved implant surface depths and widths in the range of 8 to 12 μm appear to regulate epithelial, fibroblastic, and osteoblastic cellular migration and orientation across these topographically altered surfaces.[13,15,16,19–22] A recent prospective proof-of-principle human study demonstrated that these configured 8- and 12-μm microgrooves placed on the collar of dental implants allowed direct supracrestal connective tissue attachment to the implant collar.[15] Abutment surface modifications may also be effective in preventing commonly observed crestal bone loss, much like what has been shown with implant surface modifications.[22] Previous research examined multiple abutment-related variables affecting

peri-implant and peri-abutment soft tissue attachments important in determining subsequent peri-implant bone levels.[12,23–29] Results suggest that surface characteristics of abutment components affect the epithelial, fibroblastic, and osteoblastic cellular behavior at the implant-abutment interface.

The current study dramatically underscores the effects that three-dimensional surface geometry can have on cellular behavior at the abutment-tissue interface. The presence of the 0.7-mm laser-ablated microchanneled zone consistently enabled intense fibroblastic activity to occur on the abutment-grooved surface, resulting in a dense interlacing complex of connective tissue fibers oriented perpendicular to the abutment surface that served as a physiologic barrier to apical JE migration. As a consequence of inhibiting JE apical migration, crestal bone resorption in groups A and B was prevented. Significantly, in two cases, bone regeneration coronal to the IAJ and onto the abutment surface occurred, completely eliminating the negative sequelae of the IAJ microgap.

In contrast, group C and D abutments, devoid of laser-ablated microgrooved surfaces, exhibited little evidence of robust fibroblastic activity at the abutment-tissue interface. A long JE extended along the abutment and implant collar surfaces, preventing formation of the physiologic connective tissue barrier and causing crestal bone resorption. Parallel rather than functionally oriented perpendicular connective tissue fibers apposed the abutment-implant surfaces.

Conclusions

The current proof-of-principle preclinical study suggests that carefully designed implant surface modifications may effectively prevent what often is perceived as either physiologic or inevitable crestal bony "dieback" following abutment connection. The results suggest that the 1.5 to 2.0 mm of crestal bone loss following abutment connection to accommodate the needed space for the connective tissue component of the biologic width may in fact not be a physiologically inevitable event. The study also suggests that a change may be required in how implant abutments are perceived and managed clinically. However, microgrooved surface abutments, while showing intriguing and thought-provoking results and insights, should be evaluated in a human study to verify the current results. Additionally, the question of whether the beneficial soft and hard tissue effects induced by this surface can be maintained with repetitive manipulation of the implant-abutment interface should also be evaluated.

Acknowledgments

References

1. Berglundh T, Lindhe J. Dimension of the periimplant mucosa. Biological width revisited. J Clin Periodontol 1996;23:971–973.

2. Hermann JS, Cochran DL, Nummikoski PV, Buser D. Crestal bone changes around titanium implants. A radiographic evaluation of unloaded nonsubmerged and submerged implants in the canine mandible. J Periodontol 1997;68:1117–1130.

3. Hermann JS, Buser D, Schenk RK, Higginbottom FL, Cochran DL. Biologic width around titanium implants. A physiologically formed and stable dimension over time. Clin Oral Implants Res 2000;11:1–11.

4. Hermann JS, Schoolfield JD, Nummikoski PV, Buser D, Schenk RK, Cochran DL. Crestal bone changes around titanium implants: A methodologic study comparing linear radiographic with histometric measurements. Int J Oral Maxillofac Implants 2001;16:475–485.

5. Quirynen M, Naert I, van Steenberghe D, Nys L. A study of 589 consecutive implants supporting complete fixed prostheses. Part I: Periodontal aspects. J Prosthet Dent 1992;68:655–663.

6. van Steenberghe D, Lekholm U, Bolender C, et al. Applicability of osseointegrated oral implants in the rehabilitation of partial edentulism: A prospective multcenter study on 558 fixtures. Int J Oral Maxillofac Implants 1990;5:272–281.

7. Richter EJ. Basic biomechanics of dental implants in prosthetic dentistry. J Prosthet Dent 1989;61:602–609.

8. Piattelli A, Vrespa G, Petrone G, Iezzi G, Annibali S, Scarano A. Role of the microgap between implant and abutment: A retrospective histologic evaluation in monkeys. J Periodontol 2003;74:346–352.

9. Quirynen M, van Steenberghe D. Bacterial colonization of the internal part of two-stage implants. An in vivo study. Clin Oral Implants Res 1993;4:158–161.

10. Quirynen M, Bollen CM, Eyssen H, van Steenberghe D. Microbial penetration along the implant components of the Brånemark system. An in vitro study. Clin Oral Implants Res 1994;5:239–244.

11. Ericcson I, Persson LG, Berglundh T, Marinello CP, Lindhe J, Klinge B. Different types of inflammatory reactions in peri-implant soft tissues. J Clin Periodontol 1995;22:255–261.

12. Abrahamsson I, Berglundh T, Lindhe J. The mucosal barrier following abutment dis/reconnection. An experimental study in dogs. J Clin Periodontol 1997;24:568–572.

13. Weiner S, Simon J, Ehrenberg DS, Zweig B, Ricci JL. The effects of laser microtextured collars upon crestal bone levels of dental implants. Implant Dent 2008;17:217–228.

14. Alexander H, Ricci JL, Hrico GJ. Mechanical basis for bone retention around dental implants. J Biomed Mater Res B Appl Biomater 2009;88:306–311.

15. Nevins M, Nevins ML, Camelo M, Boyesen JL, Kim DM. Human histologic evidence of a connective tissue attachment to a dental implant. Int J Periodontics Restorative Dent 2008;28:111–121.

16. Soboyejo WO, Nemetski B, Allameh S, Marcantonio N, Mercer C, Ricci J. Interactions between MC3T3-El cells and textured Ti6Al4V surfaces. J Biomed Mater Res 2002;62:56–72.

17. Listgarten MA, Lang NP, Schroeder HE, Schroeder A. Periodontal tissues and their counterparts around endosseous implants. Clin Oral Implants Res 1991;2:1–19.

18. Buser D, Weber HP, Donath K, Fiorellini JP, Paquette DW, Williams RC. Soft tissue reactions to non-submerged unloaded titanium implants in beagle dogs. J Periodontol 1992;63:225–235.

19. Ellingsen JE. Surface configurations of dental implants. Periodontol 2000 1998;17:36–46.

20. Boyan BD, Dean DD, Lohmann CH, Cochran DL, Sylvia VL, Schwartz Z. The titanium bone cell interface in vitro: The role of the surface in promoting osseointegration. In: Brunette DM, Tengvall P, Textor M, Thomson P (eds). Titanium in Medicine. Berlin: Springer-Verlag, 2001:561–585.

21. Frenkel SR, Simon J, Alexander H, Dennis M, Ricci JL. Osseointegration on metallic implant surfaces: Effects of microgeometry and growth factor treatment. J Biomed Mater Res 2002;63:706–713.

22. Pecora GE, Ceccarelli R, Bonelli M, Alexander H, Ricci JL. Clinical evaluation of laser microtexturing for soft tissue and bone attachment to dental implants. Implant Dent 2009;18:57–66.

23. Abrahamsson I, Berglundh T, Sekino S, Lindhe J. Tissue reactions to abutment shift: An experimental study in dogs. Clin Implant Dent Relat Res 2003;5:82–88.

24. Welander M, Abrahamsson I, Berglundh T. The mucosal barrier at implant abutments of different materials. Clin Oral Implants Res 2008;19:635–641.

25. Welander M, Abrahamsson I, Berglundh T. Subcrestal placement of two-part implants. Clin Oral Implants Res 2009;20:226–231.

26. Zitzmann NU, Abrahamsson I, Berglundh T, Lindhe J. Soft tissue reactions to plaque formation at implant abutments with different surface topography. An experimental study in dogs. J Clin Periodontol 2002;29:456–461.

27. Abrahamsson I, Berglundh T, Glantz PO, Lindhe J. The mucosal attachment at different abutments. An experimental study in dogs. J Clin Periodontol 1998;25:721–727.

28. Moon IS, Berglundh T, Abrahamsson I, Linder E, Lindhe J. The barrier between the keratinized mucosa and the dental implant. An experimental study in the dog. J Clin Periodontol 1999;26:658–663.

29. Abrahamsson I, Zitzmann NU, Berglundh T, Linder E, Wennerberg A, Lindhe J. The mucosal attachment to titanium implants with different surface characteristics: An experimental study in dogs. J Clin Periodontol 2002;29:448–455.